Published in final edited form as:
Neuroscience. 2014 July 25; 273: 39–51. doi:10.1016/j.neuroscience.2014.04.060.

Activation of the ACE2/Ang-(1-7)/Mas pathway reduces oxygen-glucose deprivation induced tissue swelling, ROS production, and cell death in mouse brain with angiotensin II overproduction

Jiaolin Zheng[a,b], **Guangze Li**[c], **Shuzhen Chen**[a], **Ji Chen**[a], **Joshua Buck**[a], **Yulan Zhu**[b], **Huijing Xia**[d], **Eric Lazartigues**[d], **Yanfang Chen**[a,+], and **James E. Olson**[c,e,+]

[a]Department of Pharmacology and Toxicology, Wright State University Boonshoft School of Medicine

[b]Department of Neurology, Second Affiliated Hospital, Harbin Medical University, China

[c]Department of Emergency Medicine, Wright State University Boonshoft School of Medicine

[d]Department of Pharmacology, Louisiana State University Health Sciences Center

[e]Department of Neuroscience Cell Biology and Physiology, Wright State University Boonshoft School of Medicine

Abstract

We previously demonstrated that mice which overexpress human renin and angiotensinogen (R+A+) show enhanced cerebral damage in both *in vivo* and *in vitro* experimental ischemia models. Angiotensin converting enzyme 2 (ACE2) counteracts the effects of angiotensin (Ang-II) by transforming it into Ang-(1-7), thus reducing the ligand for the AT1 receptor and increasing stimulation of the Mas receptor. Triple transgenic mice, SARA, which specifically overexpress ACE2 in neurons of R+A+ mice were used to study the role of ACE2 in ischemic stroke using oxygen and glucose deprivation (OGD) of brain slices as an *in vitro* model. We examined tissue swelling, the production of reactive oxygen species (ROS), and cell death in cerebral cortex (CX) and the hippocampal CA1 region during OGD. Expression levels of NADPH oxidase isoforms, Nox2 and Nox4 were measured using western blots. Results show that SARA mice and R+A+ mice treated with the Mas receptor agonist Ang-(1-7) had less swelling, cell death, and ROS production in CX and CA1 areas compared to those in R+A+ animals. Treatment of slices from SARA mice with the Mas antagonist A779 eliminated this protection. Finally, western blots revealed less Nox2 and Nox4 expression in SARA mice compared with R+A+ mice both before and after OGD. We suggest that reduced brain swelling and cell death observed in SARA animals exposed to OGD results from diminished ROS production coupled with lower expression of

[+]corresponding authors: Yanfang Chen: Department of Pharmacology and Toxicology, Wright State University Boonshoft School of Medicine, 207 Health Sciences Building, 3640 Colonel Glenn Highway, Dayton, Ohio, 45435, Phone: 937-775-2168, yanfang.chen@wright.edu. James Olson: Department of Emergency Medicine, Wright State University Boonshoft School of Medicine, Cox Institute, 3525 Southern Boulevard, Kettering, Ohio, 45429, Phone: 937-395-8839, james.olson@wright.edu.

NADPH oxidases. Thus, the ACE2/Ang-(1-7)/Mas receptor pathway plays a protective role in brain ischemic damage by counteracting the detrimental effects of Ang-II-induced ROS production.

Keywords

cerebral cortex; hippocampus; NADPH oxidase; brain edema; stroke; hypertension

1. INTRODUCTION

Hypertension remains a prevalent condition in adults and contributes to significant mortality and morbidity [49, 60, 64]. Specifically, hypertension is a risk factor for hemorrhagic and ischemic stroke [21, 83] and is associated with increased severity of brain injury and hemorrhagic transformation in stroke patients [3, 16, 66, 73]. Essential hypertension can result from increased levels of circulating vasoconstrictors and other hormones such as angiotensin (Ang-II), an active product of the renin-angiotensin system (RAS). The RAS also is present in the central nervous system (CNS) [82] and has been shown to have a variety of functions in physiology and pathophysiology including learning and memory, development, thirst, regulation of blood pressure and blood flow, apoptosis, and neurodegeneration [87, 88].

Pharmacological and genetic manipulation of the RAS in the CNS can influence outcomes following stroke [13, 15, 39]. Inhibition of angiotensin receptors confers protection in ischemic stroke beyond that due to reduced blood pressure [61]. Our previous studies showed that transgenic mice overexpressing human renin and angiotensinogen (R+A+) had increased tissue swelling during oxygen-glucose deprivation (OGD) and increased subsequent cell death; both of which were reduced by contemporaneous inhibition of Ang-II/AT1 receptors [13]. Another component of the RAS system, angiotensin-converting enzyme 2 (ACE2), has been identified as a negative regulator of the pro-hypertensive actions of Ang-II [70, 90]. ACE2 is a membrane-bound carboxymonopeptidase that metabolizes Ang-II to the heptapeptide Ang-(1-7) which then activates Mas receptors [71]. Central administration of Ang-(1-7) reduces brain damage and improves neurological outcome in an animal model of ischemic stroke [57] possibly mediated by anti-inflammatory actions [67]. As a negative regulator of the RAS, ACE2 over activation or expression also may have therapeutic effects on ischemic stroke [57]. While clinical studies show strong relationships between isoforms of ACE2 and the risk for hypertension [62] and brain ischemic stroke [12], the role of ACE2 in the mitigation of ischemic stroke injury and its mechanisms of action remain poorly understood.

There is considerable evidence that activation of the Ang-II receptor, AT1, in a variety of tissues leads to increased production of reactive oxygen species (ROS) mediated by NADPH oxidase (Nox) [18, 19, 27, 33, 55, 63, 85, 94]. Nox1, Nox2 and Nox4 are the predominant isoforms in neurons of the brain [35, 36, 78, 81], and play numerous roles in physiological cell signaling as well as for pathogenesis of brain injury [6, 44, 45, 47, 84]. Nox2-deficient mice have reduced infarct volumes and in wild type animals Nox4 is upregulated following stroke [81]. In addition, activation of the counteracting Mas receptor signaling by Ang-(1-7) can decrease ROS production and reduce tissue damage due to mechanical insult [8, 54, 89]. We hypothesize that in ischemic stroke, increased ROS production and resulting cell injury mediated by the

Ang-II/AT1 receptor signaling pathway is antagonized by activation of the ACE2/Ang-(1-7)/Mas receptor pathway. To test this hypothesis, we evaluated tissue swelling, ROS production, and cell death in the cerebral cortex and hippocampus in brain slices subjected to ischemic conditions induced by OGD. To evaluate the separate roles of these antagonistic pathways, we used mice which overexpress human renin and angiotensinogen in all tissues (R+A+) and SARA mice, a triple-transgenic model obtained by breeding R+A+ mice with syn-hACE2 animals overexpressing ACE2 specifically in neurons of the CNS [89].

2. EXPERIMENTAL PROCEDURES

2.1. Materials

Salts and other chemicals were obtained from Fischer Scientific (Pittsburgh, PA). Losartan was purchased from Sigma-Aldrich (St. Louis, MO). The heptapeptide Ang-(1-7) and the Mas receptor inhibitor A779 were obtained from Bachem (Torrance, CA). Propidium iodide and dihydroethedium were purchased from Life Technologies (Grand Island, NY). Complete Mini protease inhibitor and lysis buffer for protein extraction came from Roche Diagnostics Corporation (Indianapolis, IN). The Bradford protein analysis kit and precast polyacrylamide gels (Cat #456-1034) were obtained from Bio-Rad Laboratories (Hercules, CA). Primary antibodies for β-actin were purchased from Sigma-Aldrich (St. Louis, MO) and rabbit polyclonal antibodies for Nox2 and Nox4 came from Abcam (Cambridge, MA). Jackson Immunoresearch Laboratories (West Grove, PA) provided HRP-conjugated donkey anti-rabbit IgG antibody. ECL reagent was purchased from Cell Signaling (Danvers, MA).

2.2. Animals

All procedures involving animals were approved by the Laboratory Animal Care and Use Committee of Wright State University and conformed to the NIH Guide for the Care and Use of Laboratory Animals. Founder mice for generating transgenic mice were obtained from Dr. Eric Lazartigues (Louisiana State University Health Sciences Center, New Orleans). Male R+A+ individuals which overexpress renin and angiotensinogen (R+A+) [58] were bred with heterozygous transgenic females which constitutively express angiotensin converting enzyme 2 (ACE2+) in neurons of the CNS [24]. Their offspring were genotyped as previously described [43] to determine animals that were R+A+ double transgenic or R+A+ plus ACE2+ triple transgenic (SARA). Animals were maintained on a 12 hour light/dark cycle and provided access to food and water *ad libitum*.

2.3. Brain Slice Preparation

Brain slices were prepared from R+A+ and SARA mice as previously described [13]. Following rapid decapitation of the animal, brains were dissected from the cranium, mounted on a block of agar with cyanoacrylate cement, and sectioned into 400 μm-thick coronal slices using a Series 1000 Vibratome Section System (Technical Products, Inc., St. Louis, MO). Brain slices were incubated in control artificial cerebrospinal fluid (aCSF) bubbled with 95% O_2 plus 5% CO_2 at room temperature for 1–2 hr. The aCSF consisted of 124 mM NaCl, 3.5 mM KCl, 2 mM $CaCl_2$, 1 mM $MgSO_4$, 1 mM NaH_2PO_4, 26 mM $NaHCO_3$, and 10 mM glucose. After the room temperature incubation, slices were transferred to a Haas interface-type recording stage (Harvard Apparatus, Holliston, MA) and

perfused for 30 min with aCSF at 35° C under a humidified atmosphere of 95% O_2 plus 5% CO_2.

2.4. Oxygen and Glucose Deprivation (OGD)

Some slices were exposed to OGD as an *in vitro* model of brain ischemia while other slices remained in control aCSF conditions. For OGD treatment, the perfusion solution was changed to 35° C aCSF which had been bubbled with 95% N_2 plus 5% CO_2 and which contained no glucose. Simultaneous with this change in perfusion solution, the humidified gas mixture flowing over the slice was changed to 95% N_2 plus 5% CO_2. Control or OGD conditions were maintained for 30 min. For some experiments, the AT1 receptor antagonist losartan (20 μM), the Mas receptor inhibitor A779 (10 μM), or the Mas receptor agonist Ang-(1-7) (10 μM) was added to the perfusing aCSF solutions at the start of OGD exposure.

2.5. Assessment of Tissue Swelling

Tissue swelling as a measure of brain edema was determined indirectly as we and others previously described [5, 9, 51] by measuring the intrinsic optical signal (IOS) defined as the intensity of transmitted light during OGD treatment expressed as a percent of the intensity measured prior to the start of OGD [5]. Slices were transilluminated using a DC-regulated halogen lamp which delivered white light to the recording stage via a randomized fiber optic bundle. Images of the slice were acquired as a single standard NTSC video frame using a fixed gain video camera and 8-bit image processor board (DT2867, Data Translation, Inc., Marlboro, MA). By capturing images of dry laboratory tissue paper, this image acquisition system was found to have a linear intensity drift of −0.1% per hour with a standard deviation of 0.05% about this drift line. At the beginning of each experiment, the light source was adjusted such that the average light intensity transmitted through the slice was in the middle of the image acquisition system's dynamic range (0–255 units). Then images were acquired at 60 sec intervals. Image analysis was subsequently performed using NIH-Image and ImageJ software. Regions of interest (ROI) were defined in *stratum radiatum* of the hippocampal CA1 area and in an equivalent area in the center of the adjacent cerebral cortex. The average light intensities in these ROIs were calculated for each image and then normalized to the average ROI intensity measured immediately prior to the start of OGD exposure. In addition, regional IOS was displayed by creating a pseudo-color image with red indicating increases in light intensity and blue indicating decreases in light intensity.

2.6. Measurement of Reactive Oxygen Species Production

Dihydroethidium (DHE) was used to evaluate the generation of ROS products in slices exposed to control conditions or OGD. After the initial 30 min perfusion with control aCSF at 35° C, slices in control conditions or during OGD were perfused with 10 μM DHE for 30 min. During DHE treatment the light source illuminating the slice and other room lights were turned off. Thus, no IOS measurements were made on slices used for studies of ROS production. Non-fluorescent DHE molecules freely penetrate cell membranes where they may be oxidized to ethidium by ROS [10, 32, 86]. Ethidium fluorescence then is greatly enhanced after binding to endogenous nucleic acids. After this treatment, slices were fixed for at least 1 hr with 4% paraformaldehyde in staining buffer (SB) consisting of 137 mM

NaCl plus 10 mM Na_2HPO_4 (pH 7.4). They then were washed for 20 min with SB and mounted on glass slides under coverslips using Fluoro-Gel aqueous mounting medium (Electron Microscopy Services, Hatfield, PA). Photographs of the pyramidal cell layer in the middle of the CA1 region and in the center of the adjacent cerebral cortex were captured under epifluorescence illumination. To eliminate bias in selecting the region of interest photographed for each brain region, we first identified the general brain area in the slice using a 10× objective. Then the objective was switched to 40×, the image focused without further manipulation of the stage, and a single image acquired. The number of DHE-positive cells per microscope field was counted using ImageJ software after subtracting background fluorescence. Data representing cell density are expressed as the number of cells per microscope field.

2.7. Evaluation of Cell Death

Cell death was determined using propidium iodide (PI) staining of slices used for measurements of IOS. Following a 30 min exposure to control or OGD conditions, slices were incubated with 20 μg/ml PI in aCSF for 15 min at room temperature and then fixed overnight with 4% paraformaldehyde in SB. Slices were washed with SB and mounted under coverslips with Fluoro-Gel. PI-positive cells were visualized using laser confocal microscopy and digital images of the CA1 region and cerebral cortex captured for analysis using an unbiased selection procedure to identify regions of interest as described above. The approximate surface of the slice was found by adjusting the focus. Then, to avoid the influence of cell injury at the slice surface caused during slice preparation, we counted only PI-positive nuclei which were situated in a single plane approximately 80–90 μm below the slice surface. The cell density of PI-positive cells is expressed as the number of cells per microscope field.

2.8. Expression levels of Nox2 and Nox4

Following a 30 min exposure to control or OGD conditions, slices were removed from the perfusion chamber following measurements of IOS and homogenized on ice in lysis buffer containing Complete Mini protease inhibitors and EDTA. Total protein content of the solution was determined using the Bradford protein assay. Equal amounts (50 μg) of protein were loaded into lanes of a 10% precast polyacrylamide gel, separated by electrophoresis, and then electrotransferred onto a PVDF membrane. Membranes were blocked for 1 hour in 5% non-fat dry milk and were probed with primary monoclonal rabbit anti-mouse β-actin (1:4000), polyclonal rabbit anti-mouse Nox2 (1:1000) or polyclonal rabbit anti-mouse Nox4 (1:500) overnight at 4° C. Membranes then were washed and incubated with HRP-conjugated donkey anti-rabbit IgG (1:40,000). Blots were probed using enhanced chemiluminescence with ECL reagent and visualized using a Fuji film image analyzer (Molecular Dynamics Image Quant, Sunnyvale, CA). Bands for β-actin, Nox2, and Nox4 were visualized at mean ± SD apparent molecular weights of 47.0 ± 1.3 kDa, 61.6 ± 2.4 kDa, and 60.7 ± 2.2 kDa, respectively (N=8).

2. 9. Data Analysis

A power analysis was performed to determine the number of animals needed for these studies. Based on results from our previous report [13], the OGD-induced IOS in R+A+ and

wild type animals differed by 34% with a pooled standard deviation of 16%. This yielded a requirement of 3 animals per group to detect a similar difference between the final IOS values from the transgenic animals used in the present study for $\alpha = 0.05$ and $\beta = 0.80$. Similarly, we previously found that the number of cell counts for PI-positive cells following OGD decreased by 78% with pharmacological AT1 receptor inhibition. From this we calculated a requirement of only 2 animals to find this magnitude of effect for $\alpha = 0.05$ and $\beta = 0.80$. IOS data are displayed as the mean ± SEM and were log-transformed before being analyzed using ANOVA followed by Dunnett's test for multiple comparisons. Cell count data were analyzed with the Mann-Whitney, Kruskal-Wallis, and Student-Neuman-Keuls tests as appropriate to evaluate differences between experimental groups. Nox expression data were log-transformed and then analyzed using two-way ANOVA with animal genotype and treatment as independent variables followed by Neuman-Keuls multiple comparison tests. Percent changes in Nox expression levels were analyzed by Neuman-Keuls test. Significance was indicated for $p < 0.05$.

3. Results

3.1. OGD-induced tissue swelling is reduced by activation of the ACE2/Ang-(1-7)/Mas axis or by inhibition of the AT1 receptor

The intensity of light transmission through slices stabilized during the initial 30 min of perfusion with control aCSF (Figure 1.B.). Similar to our previous results [13], within 10 min of the start of OGD exposure, IOS increased significantly in both brain regions with the hippocampus showing a greater increase than that observed in cerebral cortex (Figures 1.A and 1.B.). The IOS of cerebral cortex from SARA animals appeared to change little during the first 5 min of OGD while IOS from R+A+ animals was already significantly different from the initial value by this time point. IOS from both animal groups continued to increase throughout the period of OGD exposure; however, the increase was significantly greater for slices from R+A+ animals compared with slices from SARA animals. After 30 min of OGD, IOS measured in the cerebral cortex and hippocampus of slices from SARA animals was 39% and 68% of that measured in slices from R+A+ animals (Figure 1.C.). As previously reported, treating slices with 20 μM losartan significantly attenuated IOS during OGD to values not different than 100% [13]. In addition, treating slices from R+A+ animals with the Mas receptor agonist Ang-(1-7) (10 μM) reduced the magnitude of IOS after 30 min of OGD in both brain regions. The average magnitude of IOS response was greater for SARA animals treated with the Mas receptor antagonist A779 (10 μM); however the increase in each brain region was not statistically different.

3.2. OGD-induced ROS production is reduced by activation of the ACE2/Ang-(1-7)/Mas axis or by inhibition of the AT1 receptor

Following perfusion with control aCSF, a small number of cells stained positive for DHE in cerebral cortex and the hippocampal CA1 region of slices from R+A+ and SARA animals (Figure 2.B.). The number of DHE-positive cells was not significantly different for each animal genotype under control perfusion conditions. Exposure to OGD significantly increased the number of DHE-positive cells in both animal groups. Nevertheless, the number of DHE-positive cells per microscope field in cerebral cortex was significantly

greater in brain slices from R+A+ animals compared with the number observed in brain slices from SARA animals. Losartan treatment during OGD significantly decreased the number of DHE-positive cells in both brain regions of R+A+ and SARA animals to levels that were not significantly different from those measured in slices from animals of the same genotype without OGD exposure.

3.3. OGD-induced cell death is reduced by activation of ACE2/Ang-(1-7)/Mas axis or by inhibition of the AT1 receptor

Slices from both R+A and SARA animals exposed to control aCSF showed low intensity fluorescence in a small number of cells (Figure 3.A.). For each genotype, a significantly greater number of cells appeared brightly PI-positive following 30 min of OGD. Compared with slices from R+A+ animals, slices from SARA mice had fewer PI-positive cells per microscope field in the cerebral cortex and CA1 region following OGD exposure (Figure 3.B.). In addition, treating slices from R+A+ animals with Ang-(1-7) reduced the PI-positive cell count in both brain regions while treating slices from SARA animals with A779 significantly increased the PI-positive cell count in cerebral cortex. Finally, adding the Ang-II receptor antagonist, losartan (20 μM) to slices from SARA animals during OGD significantly reduced the number of DHE-positive cells in cerebral cortex and hippocampal CA1 region.

3.4. Nox2 and Nox4 expression levels are reduced by neuronal ACE2 expression

Both Nox2 and Nox4 were expressed in brain slices from wild type, R+A+, and SARA animals (Figure 4A and 4B). For control slices from R+A+ animals, the relative expression of Nox2 was similar while the relative expression of Nox4 was elevated compared with that measured in slices from wild type animals. We observed lower expression levels for Nox2 and Nox4 in control slices from SARA mice compared with those measured in slices from R+A+ mice. For slices from all genotypes, relative expression levels of Nox2 increased following OGD exposure; however, the percent increase relative to control slices was smaller in slices from SARA animals compared with that measured in slices from wild type and R+A+ mice (Figure 4C). Additionally, the relative expression of Nox2 in slices from SARA animals remained significantly below that measured in slices from R+A+ animals. For Nox4, OGD exposure increased expression in slices from wildtype and SARA mice, but not in slices from R+A+ animals. The percent increase in Nox4 expression in slices from SARA animals following OGD was similar to that observed for slices from wild type mice.

4. DISCUSSION

These studies elucidate interactions between components of the brain RAS system which impact the magnitude of tissue damage during ischemic conditions in an animal model of essential hypertension. Because these studies were performed using *in vitro* brain preparations, the effects we observed by genetically and pharmacologically manipulating RAS pathways are independent of their effect on blood pressure or cerebrovascular tone. First, we found that inhibition of the AT1 receptor with losartan reduces or eliminates tissue swelling during OGD in slices from SARA animals which constitutively overexpress human renin and angiotensinogen and also overexpress ACE2 selectively in neurons. These results

expand upon our previous studies which showed that treatment with losartan reduced tissue swelling in slices from wild type and R+A+ animals exposed to OGD [13]. Second, the current study further extends results from our previous investigation by demonstrating that losartan reduces cell death in brain slices from SARA animals as well as in brain slices from R+A+ mice. Third, our data demonstrate that ACE2 overexpression in neurons reduces cell damage from OGD in cerebral cortex and hippocampus. Compared with brain tissue from R+A+ animals, the brain slices of SARA animals developed less tissue swelling, as evidenced by a smaller change in IOS, and had a lower density of PI-positive cells after a 30 min OGD treatment. Finally, we observed decreased levels of ROS production and lower expression levels of Nox2 following OGD exposure in slices from SARA animals compared with those measured in R+A+ animals. Thus, we propose that the decrease in cellular injury following OGD in slices from animals with neuronal ACE2 overexpression results from decreased oxidative stress mediated by the Ang-(1-7)/Mas receptor pathway. Although we did not measure Nox expression levels separately in hippocampus and cerebral cortex in this initial study, we expect there were comparable responses of these enzymes to OGD in each region since we observed similar qualitative changes in tissue swelling, cell death, and ROS production in cerebral cortex and hippocampus.

The hypothesized role of the Ang-(1-7)/Mas receptor pathway for brain protection is strongly supported by our results showing that exposure of slices from R+A+ animals to the Mas agonist Ang-(1-7) decreases OGD-induced injury while exposing slices from SARA animals to the Mas inhibitor A779 increases oxidative stress and cell injury following OGD. Activation of Mas receptors with Ang-(1-7) and inhibition of AT1 receptors with losartan both ameliorate OGD-induced injury. However, we cannot infer a relative efficiency of these two signaling pathways as our studies were designed and statistically powered only to compare results from R+A+ animals with those from SARA animals. Interpretation of these pharmacological studies also must take into account recent reports which suggest that part of the beneficial effects of AT1 receptor blockers are mediated through enhanced activity of ACE2 or the Ang-(1-7)/Mas signaling pathway [37, 40, 59]. Blockade of the AT1 receptor increases Ang-II levels making it more available for conversion into Ang-(1-7) by ACE2. Accordingly it is not surprising that the combination of an AT1 receptor blocker with enhanced expression of ACE2 would provide a stronger benefit than application of Ang-(1-7).

In many cell systems, the Ang-(1-7)/Mas intracellular signaling pathway is functionally opposed to the actions of the Ang-II/AT1 receptor pathway [23, 25, 52, 90]. Our data are consistent with this relationship in that overexpression of ACE2 in SARA mice appears to reverse the effects of AT1 receptor activation that results from overproduction of Ang-II in the R+A+ animals. This reversal may result from ACE2-mediated conversion of Ang-I and Ang-II into Ang-(1-9) and Ang-(1-7), respectively; peptides that are inactive at the AT1 receptor. However, we conclude that the Ang-II/AT1 receptor pathway is not completely inactive in SARA animals during OGD since losartan reduces cell death and levels of oxidative stress in slices from these mice. While the data support our hypothesis that activation of the Mas receptor by Ang-(1-7) is responsible for the reduction in cell death in brain slices from SARA animals following OGD, the cellular location of the Mas receptor which mediates this neuroprotection is not clear nor is its mechanism of action. Potentially,

Mas receptor activation reduces ROS production in this animal model as has been observed in cultured neuroblastoma cells, rat autonomic system, vascular smooth muscle and adipocytes from mouse [8, 89].

Various isoforms of NADPH have been identified in neurons and glial cells of the CNS [11, 14, 65, 68, 93] and previous clinical and animal studies have shown their importance for pathogenesis of injury following ischemia [48, 53]. Compared with slices from wild type mice in control conditions, slices from R+A+ animals had similar expression levels of Nox2, but elevated expression levels of Nox4. A different expression pattern was seen in slices from SARA mice where Nox2 levels were decreased while Nox4 levels were similar to those measured in wild type mice. We found Nox2 and Nox 4 expression levels were increased in slices from wild type mice within 30 min of initiating the OGD treatment. A similarly rapid increase in Nox expression levels occur in human endothelial cells following atrial natriuretic peptide treatment due to increased transcription to mRNA [28]. Once expressed the activity of Nox4 can persist for 24 hr [72].

The reduction in the density of DHE-positive cells with losartan treatment following OGD indicates that the AT1 receptor is coupled to ROS production in mouse brain. Ang-II activation of ROS production has been observed in a number of tissues including brain. Previously, Griendling et al. demonstrated that activation of the AT1 receptor in cultured smooth muscle cells increases ROS production by activating NADPH oxidase to produce superoxide [31]. Others have shown that the actions of Ang-II in the CNS are mediated by superoxide production or by increased activity of specific Nox enzymes [85, 95, 96]. Similarly pharmacologic inhibition of the AT1 receptor can limit oxidative stress in cardiac tissue and brain [42, 69, 77]. Our results suggest that increased ROS production following OGD is related to elevated expression levels of both Nox2 and Nox4 isoforms. Conversely we suggest that brain cell protection in slices from SARA mice follows from lower expression levels of Nox2 and Nox4 after OGD compared with those measured in slices from R+A+ animals and this lower expression of Nox isoforms results in decreased ROS production. OGD induces a smaller percent change in Nox2 expression in slices from SARA mice compared with the percent change measured in R+A+ animals. Thus the decreased expression of Nox isoforms in slices from SARA mice is a consequence of both lower control levels of Nox activity and a limited increase in Nox expression during OGD. In contrast, the OGD-induced percent change in Nox4 expression is greater in SARA animals while the relative expression level of Nox4 is similar to that observed in slices from R+A+ mice. These results suggest ACE2 mediates its effect on ROS production predominantly via modulation of Nox2 expression. We previously reported OGD-induced cell death is greater in brain slices from R+A+ mice compared to that found in slices from wild type mice [13]. However, levels of Nox2 and Nox4 expression in R+A+ mice following OGD are similar to those measured in slices from wild type mice suggesting changes in Nox activity rather than expression levels are affecting OGD-induced cell death in R+A+ mice. Mechanisms by which activation of AT1 and Mas receptors may alter Nox isoform expression in this animal model of ischemic stroke are unknown.

Tissue swelling as a result of cytotoxic or vasogenic edema is commonly observed following clinical stroke and in *in vivo* and *in vitro* models of hypoxia/ischemia [46, 56, 74, 92]. In

ischemia, the magnitude of the change in tissue water content is dependent on the degree of brain injury [56]. Changes in brain extracellular or intracellular water content as a result of exposure to aniso-osmotic, hypoxic, or ischemic conditions alter the optical properties of the tissue, measured here as the IOS [1, 9, 30, 41]. In the present studies, we found a consistent increase in IOS in slices from SARA mice during OGD, similar to our previous studies using brain slices from wild type and R+A+ mice [13]. We suggest these responses represent swelling of the brain tissue, but cannot determine to what degree the edema is due to changes in volumes of extracellular or intracellular spaces. Although we find quantitative differences in IOS during OGD for slices from R+A+ and SARA animals, our measurements of PI-positive and DHE-positive cell densities cannot be corrected for tissue swelling since the relation between IOS and tissue volume are not known for this animal model. By itself, the smaller degree of tissue swelling during OGD seen for slices from SARA animals would result in a higher cell density compared with slices from R+A+ animals. Thus, the quantitative difference in PI-positive cell density between slices from SARA and R+A+ animals is likely to be greater than reported in Figure 3.

These investigations do not indicate whether neurons or glial cells are responsible for the tissue volume changes measured by the IOS, which cell type has increased ROS production, or which cells die during OGD. IOS is a general measure of tissue swelling and can result from changes in light reflection, scattering, and absorption [1, 22] and quantitatively may depend on slice configuration along the optical axis between the light source and imaging device [50]. IOS increases in osmotically swollen brain slices and decreases when hyperosmotic solutions are applied to cause dehydration and cellular shrinkage [4, 22, 51]. Thus, an increase in IOS is generally believed to represent swelling by both glial cells and neurons [4]. In these studies IOS increased by approximately 25% to 30% during OGD, a value comparable to our previous studies of rat brain slices treated with 200 mOsm aCSF [51] but considerably higher than the 4%-6% change in response to exogenous ROS treatment (2 mM H_2O_2) [79]. However during OGD and associated spreading depression, changes in the volume of intracellular organelles and localized swelling (beading) of neuronal dendrites also may contribute significantly to changes in light transmission [22, 80]. These latter processes may cause the persistent IOS elevation during OGD in the presence of losartan despite complete inhibition of excess ROS production and cell death by this drug.

Cellular localization of the various RAS system components which give rise to elevated ROS production and cell death during OGD also are not defined by the current studies. Astrocytes and neuroblastoma cells express Ang-II receptors [26, 34] and angiotensinogen is synthesized in neurons and astrocytes *in vivo* [76]. Certain cortical brain structures may produce some but not all of the major peptide components of the RAS system (reviewed by von Bohlen und Halbach [82]); however, in the hippocampus angiotensinogen, angiotensin, renin, and ACE are all present [91]. The AT1 and AT2 receptors for Ang-II are found throughout the hippocampus, but may be expressed regionally in cerebral cortex [29]. Previous results from our group and others show that ACE2 is distributed throughout the mouse brain and expressed in both on the cell surface and in the cytoplasm of neurons but not in glial cells [20]. SARA animals are genetically engineered to overexpress ACE2 in neurons of the CNS [24]. The differences in sensitivity we observed in cerebral cortex and hippocampus for

IOS, ROS production, and cell death may be related to the abundance and localization of the sources and targets of Ang-II and Ang-(1-7) in these brain regions. Cell-specific relations between these signaling pathways, localization of Nox enzymes, ROS production, and cell injury during ROS are currently unknown.

Clinical studies have suggested that Ang-II receptor blockers can have beneficial effects in pathological conditions beyond their effects on blood pressure alone. They may lower the risk for myocardial infarction [7], improve the treatment of patients in end stage renal disease [75], decrease the incidence of stroke [38, 61], and improve stroke outcome [2]. Because of the antagonist relations between the ACE2/Ang-(1-7)/Mas axis and the Ang-II/AT1 pathway, others have suggested that augmentation of Mas signaling by pharmacological or genetic methods also may be a means of improving outcomes in these pathological situations [17, 52]. The results of our studies support this conjecture for the treatment of stroke in patients with essential hypertension. The ultimate utility of using activators of the Ang(1-7)/Mas signaling pathway to ameliorate brain damage following stroke must await results from future clinical investigations.

Acknowledgments

This work was supported by the National Heart, Lung, and Blood Institute (HL-098637 to YC and JO; HL-093178 to EL) and the National Natural Science Foundation of China (NSFC, #81271214, #81300079).

References

1. Aitken PG, Fayuk D, Somjen GG, Turner DA. Use of intrinsic optical signals to monitor physiological changes in brain tissue slices. Methods. 1999; 18:91–103. [PubMed: 10356339]
2. Al-Nimer MS. Significant beneficial effect of AT-1 receptor blockers (sartans) in stroke. Neurosciences. 2012; 17:6–15. [PubMed: 22246005]
3. Alvarez-Sabin J, Maisterra O, Santamarina E, Kase CS. Factors influencing haemorrhagic transformation in ischaemic stroke. Lancet neurology. 2013; 12:689–705.
4. Andrew RD, Jarvis CR, Obeidat AS. Potential sources of intrinsic optical signals imaged in live brain slices. Methods. 1999; 18:185–196. 179. [PubMed: 10356350]
5. Andrew RD, MacVicar BA. Imaging cell volume changes and neuronal excitation in the hippocampal slice. Neuroscience. 1994; 62:371–383. [PubMed: 7830884]
6. Atkins CM, Sweatt JD. Reactive oxygen species mediate activity-dependent neuron-glia signaling in output fibers of the hippocampus. J Neurosci. 1999; 19:7241–7248. [PubMed: 10460230]
7. Bangalore S, Kumar S, Wetterslev J, Messerli FH. Angiotensin receptor blockers and risk of myocardial infarction: meta-analyses and trial sequential analyses of 147 020 patients from randomised trials. BMJ. 2011; 342:d2234. [PubMed: 21521728]
8. Bodiga S, Zhong JC, Wang W, Basu R, Lo J, Liu GC, Guo D, Holland SM, Scholey JW, Penninger JM, Kassiri Z, Oudit GY. Enhanced susceptibility to biomechanical stress in ACE2 null mice is prevented by loss of the p47(phox) NADPH oxidase subunit. Cardiovasc Res. 2011; 91:151–161. [PubMed: 21285291]
9. Brisson CD, Lukewich MK, Andrew RD. A distinct boundary between the higher brain's susceptibility to ischemia and the lower brain's resistance. PLoS One. 2013; 8:e79589. [PubMed: 24223181]
10. Bucana C, Saiki I, Nayar R. Uptake and accumulation of the vital dye hydroethidine in neoplastic cells. J Histochem Cytochem. 1986; 34:1109–1115. [PubMed: 2426339]
11. Case AJ, Li S, Basu U, Tian J, Zimmerman MC. Mitochondrial-localized NADPH oxidase 4 is a source of superoxide in angiotensin II-stimulated neurons. Am J Physiol Heart Circ Physiol. 2013; 305:H19–28. [PubMed: 23624625]

12. Chen DL, Zhang CJ, Fu YH, Mo YJ, Chen FR. Correlation of angiotensin-converting enzyme 2 gene polymorphisms to essential hypertension and ischemic stroke. Nan Fang Yi Ke Da Xue Xue Bao. 2010; 30:1890–1892. 1895. [PubMed: 20813695]
13. Chen S, Li G, Zhang W, Wang J, Sigmund CD, Olson JE, Chen Y. Ischemia induced brain damage is enhanced in human renin and angiotensinogen double transgenic mice. Am J Physiol (Regul Integr Comp Physiol). 2009; 297:R1526–R1531. [PubMed: 19759335]
14. Choi SH, Lee DY, Chung ES, Hong YB, Kim SU, Jin BK. Inhibition of thrombin-induced microglial activation and NADPH oxidase by minocycline protects dopaminergic neurons in the substantia nigra in vivo. J Neurochem. 2005; 95:1755–1765. [PubMed: 16219027]
15. Dai WJ, Funk A, Herdegen T, Unger T, Culman J. Blockade of central angiotensin AT(1) receptors improves neurological outcome and reduces expression of AP-1 transcription factors after focal brain ischemia in rats. Stroke. 1999; 30:2391–2398. discussion 2398–2399. [PubMed: 10548676]
16. Davis BR, Vogt T, Frost PH, Burlando A, Cohen J, Wilson A, Brass LM, Frishman W, Price T, Stamler J. Systolic Hypertension Elderly Program C. Risk factors for stroke and type of stroke in persons with isolated systolic hypertension. Stroke. 1998; 29:1333–1340. [PubMed: 9660383]
17. Der Sarkissian S, Huentelman MJ, Stewart J, Katovich MJ, Raizada MK. ACE2: A novel therapeutic target for cardiovascular diseases. Prog Biophys Mol Biol. 2006; 91:163–198. [PubMed: 16009403]
18. Didion SP, Ryan MJ, Baumbach GL, Sigmund CD, Faraci FM. Superoxide contributes to vascular dysfunction in mice that express human renin and angiotensinogen. Am J Physiol Heart Circ Physiol. 2002; 283:H1569–1576. [PubMed: 12234811]
19. Didion SP, Ryan MJ, Didion LA, Fegan PE, Sigmund CD, Faraci FM. Increased superoxide and vascular dysfunction in CuZnSOD-deficient mice. Circ Res. 2002; 91:938–944. [PubMed: 12433839]
20. Doobay MF, Talman LS, Obr TD, Tian X, Davisson RL, Lazartigues E. Differential expression of neuronal ACE2 in transgenic mice with overexpression of the brain renin-angiotensin system. Am J Physiol Regul Integr Comp Physiol. 2007; 292:R373–381. [PubMed: 16946085]
21. Elkind MS. Epidemiology and risk factors. Continuum (Minneap Minn). 2011; 17:1213–1232. [PubMed: 22810026]
22. Fayuk D, Aitken PG, Somjen GG, Turner DA. Two different mechanisms underlie reversible, intrinsic optical signals in rat hippocampal slices. J Neurophysiol. 2002; 87:1924–1937. [PubMed: 11929912]
23. Feng Y, Hans C, McIlwain E, Varner KJ, Lazartigues E. Angiotensin-converting enzyme 2 over-expression in the central nervous system reduces angiotensin-II-mediated cardiac hypertrophy. PLoS One. 2012; 7:e48910. [PubMed: 23155428]
24. Feng Y, Xia H, Cai Y, Halabi CM, Becker LK, Santos RA, Speth RC, Sigmund CD, Lazartigues E. Brain-selective overexpression of human Angiotensin-converting enzyme type 2 attenuates neurogenic hypertension. Circ Res. 2010; 106:373–382. [PubMed: 19926873]
25. Feng Y, Xia H, Santos RA, Speth R, Lazartigues E. Angiotensin-converting enzyme 2: a new target for neurogenic hypertension. Exp Physiol. 2010; 95:601–606. [PubMed: 19923158]
26. Fogarty DJ, Sanchez-Gomez MV, Matute C. Multiple angiotensin receptor subtypes in normal and tumor astrocytes in vitro. Glia. 2002; 39:304–313. [PubMed: 12203396]
27. do Franco MC, Akamine EH, Di Marco GS, Casarini DE, Fortes ZB, Tostes RC, Carvalho MH, Nigro D. NADPH oxidase and enhanced superoxide generation in intrauterine undernourished rats: involvement of the renin-angiotensin system. Cardiovasc Res. 2003; 59:767–775. [PubMed: 14499878]
28. Furst R, Brueckl C, Kuebler WM, Zahler S, Krotz F, Gorlach A, Vollmar AM, Kiemer AK. Atrial natriuretic peptide induces mitogen-activated protein kinase phosphatase-1 in human endothelial cells via Rac1 and NAD(P)H oxidase/Nox2-activation. Circ Res. 2005; 96:43–53. [PubMed: 15569826]
29. Gehlert DR, Gackenheimer SL, Schober DA. Autoradiographic localization of subtypes of angiotensin II antagonist binding in the rat brain. Neuroscience. 1991; 44:501–514. [PubMed: 1944896]

30. Gill AS, Rajneesh KF, Owen CM, Yeh J, Hsu M, Binder DK. Early optical detection of cerebral edema in vivo. J Neurosurg. 2011; 114:470–477. [PubMed: 20205509]
31. Griendling KK, Minieri CA, Ollerenshaw JD, Alexander RW. Angiotensin II stimulates NADH and NADPH oxidase activity in cultured vascular smooth muscle cells. Circulation research. 1994; 74:1141–1148. [PubMed: 8187280]
32. Gu Y, Lewis DF, Zhang Y, Groome LJ, Wang Y. Increased superoxide generation and decreased stress protein Hsp90 expression in human umbilical cord vein endothelial cells (HUVECs) from pregnancies complicated by preeclampsia. Hypertens Pregnancy. 2006; 25:169–182. [PubMed: 17065038]
33. Haugen EN, Croatt AJ, Nath KA. Angiotensin II induces renal oxidant stress in vivo and heme oxygenase-1 in vivo and in vitro. Kidney Int. 2000; 58:144–152. [PubMed: 10886559]
34. Hoffmann A, Cool DR. Angiotensin II receptor types 1A, 1B, and 2 in murine neuroblastoma Neuro-2a cells. Journal of receptor and signal transduction research. 2003; 23:111–121. [PubMed: 12680593]
35. Ibi M, Katsuyama M, Fan C, Iwata K, Nishinaka T, Yokoyama T, Yabe-Nishimura C. NOX1/NADPH oxidase negatively regulates nerve growth factor-induced neurite outgrowth. Free Radic Biol Med. 2006; 40:1785–1795. [PubMed: 16678016]
36. Infanger DW, Sharma RV, Davisson RL. NADPH oxidases of the brain: distribution, regulation, and function. Antioxid Redox Signal. 2006; 8:1583–1596. [PubMed: 16987013]
37. Ishibashi Y, Matsui T, Yamagishi S. Olmesartan Blocks Advanced Glycation End Products-induced VCAM-1 Gene Expression in Mesangial Cells by Restoring Angiotensin-converting Enzyme 2 Level. Horm Metab Res. 2013
38. Iso H, Shimamoto T, Naito Y, Sato S, Kitamura A, Iida M, Konishi M, Jacobs DR Jr, Komachi Y. Effects of a long-term hypertension control program on stroke incidence and prevalence in a rural community in northeastern Japan. Stroke. 1998; 29:1510–1518. [PubMed: 9707185]
39. Iwanami J, Mogi M, Iwai M, Horiuchi M. Inhibition of the renin-angiotensin system and target organ protection. Hypertens Res. 2009; 32:229–237. [PubMed: 19262496]
40. Iwanami J, Mogi M, Tsukuda K, Wang XL, Nakaoka H, Ohshima K, Chisaka T, Bai HY, Kanno H, Min LJ, Horiuchi M. Role of angiotensin-converting enzyme 2/angiotensin-(1-7)/Mas axis in the hypotensive effect of azilsartan. Hypertens Res. 2014
41. Joshi I, Andrew RD. Imaging anoxic depolarization during ischemia-like conditions in the mouse hemi-brain slice. J Neurophysiol. 2001; 85:414–424. [PubMed: 11152742]
42. Jung KH, Chu K, Lee ST, Kim SJ, Song EC, Kim EH, Park DK, Sinn DI, Kim JM, Kim M, Roh JK. Blockade of AT1 receptor reduces apoptosis, inflammation, and oxidative stress in normotensive rats with intracerebral hemorrhage. The Journal of pharmacology and experimental therapeutics. 2007; 322:1051–1058. [PubMed: 17538008]
43. Kao JP, Harootunian AT, Tsien RY. Photochemically generated cytosolic calcium pulses and their detection by fluo-3. J Biol Chem. 1989; 264:8179–8184. [PubMed: 2498309]
44. Kishida KT, Klann E. Sources and targets of reactive oxygen species in synaptic plasticity and memory. Antioxid Redox Signal. 2007; 9:233–244. [PubMed: 17115936]
45. Kishida KT, Pao M, Holland SM, Klann E. NADPH oxidase is required for NMDA receptor-dependent activation of ERK in hippocampal area CA1. J Neurochem. 2005; 94:299–306. [PubMed: 15998281]
46. Klatzo, I.; Suzuki, R.; Orzi, P.; Schuier, F.; Nitsch, C. Pathomechanisms of ischemic brain edema. In: Go, KG.; BA, editors. Recent Progress in the Study and Therapy of Brain Edema. Plenum Press; New York: 1984. p. 1-10.
47. Knapp LT, Klann E. Role of reactive oxygen species in hippocampal long-term potentiation: contributory or inhibitory? J Neurosci Res. 2002; 70:1–7. [PubMed: 12237859]
48. Kochanski R, Peng C, Higashida T, Geng X, Huttemann M, Guthikonda M, Ding Y. Neuroprotection conferred by post-ischemia ethanol therapy in experimental stroke: an inhibitory effect on hyperglycolysis and NADPH oxidase activation. J Neurochem. 2013; 126:113–121. [PubMed: 23350720]
49. Kountz DS. Hypertension in black patients: an update. Postgraduate medicine. 2013; 125:127–135. [PubMed: 23748513]

50. Kreisman NR, LaManna JC, Liao SC, Yeh ER, Alcala JR. Light transmittance as an index of cell volume in hippocampal slices: Optical differences of interfaced and submerged positions. Brain Res. 1995; 693:179–186. [PubMed: 8653406]
51. Kreisman NR, Olson JE. Taurine enhances volume regulation in hippocampal slices swollen osmotically. Neuroscience. 2003; 120:635–642. [PubMed: 12895504]
52. Lazartigues E, Feng Y, Lavoie JL. The two fACEs of the tissue renin-angiotensin systems: implication in cardiovascular diseases. Curr Pharm Des. 2007; 13:1231–1245. [PubMed: 17504232]
53. Li BH, Zhang LL, Zhang BB, Yin YW, Dai LM, Pi Y, Guo L, Gao CY, Fang CQ, Wang JZ, Li JC. Association between NADPH oxidase p22(phox) C242T polymorphism and ischemic cerebrovascular disease: a meta-analysis. PLoS One. 2013; 8:e56478. [PubMed: 23409188]
54. Liu C, Lv XH, Li HX, Cao X, Zhang F, Wang L, Yu M, Yang JK. Angiotensin-(1-7) suppresses oxidative stress and improves glucose uptake via Mas receptor in adipocytes. Acta Diabetol. 2012; 49:291–299. [PubMed: 22042130]
55. Lopez-Real A, Rey P, Soto-Otero R, Mendez-Alvarez E, Labandeira-Garcia JL. Angiotensin-converting enzyme inhibition reduces oxidative stress and protects dopaminergic neurons in a 6-hydroxydopamine rat model of Parkinsonism. J Neurosci Res. 2005; 81:865–873. [PubMed: 16015598]
56. MacGregor DG, Avshalumov MV, Rice ME. Brain edema induced by in vitro ischemia: causal factors and neuroprotection. J Neurochem. 2003; 85:1402–1411. [PubMed: 12787060]
57. Mecca AP, Regenhardt RW, O'Connor TE, Joseph JP, Raizada MK, Katovich MJ, Sumners C. Cerebroprotection by angiotensin-(1-7) in endothelin-1-induced ischaemic stroke. Exp Physiol. 2011; 96:1084–1096. [PubMed: 21685445]
58. Merrill DC, Thompson MW, Carney CL, Granwehr BP, Schlager G, Robillard JE, Sigmund CD. Chronic hypertension and altered baroreflex responses in transgenic mice containing the human renin and human angiotensinogen genes. J Clin Invest. 1996; 97:1047–1055. [PubMed: 8613528]
59. Ohshima K, Mogi M, Nakaoka H, Iwanami J, Min LJ, Kanno H, Tsukuda K, Chisaka T, Bai HY, Wang XL, Ogimoto A, Higaki J, Horiuchi M. Possible role of angiotensin-converting enzyme 2 and activation of angiotensin II type 2 receptor by angiotensin-(1-7) in improvement of vascular remodeling by angiotensin II type 1 receptor blockade. Hypertension. 2014; 63:e53–59. [PubMed: 24379178]
60. Osawa H, Doi Y, Makino H, Ninomiya T, Yonemoto K, Kawamura R, Hata J, Tanizaki Y, Iida M, Kiyohara Y. Diabetes and hypertension markedly increased the risk of ischemic stroke associated with high serum resistin concentration in a general Japanese population: the Hisayama Study. Cardiovasc Diabetol. 2009; 8:60. [PubMed: 19922611]
61. Padma V, Fisher M, Moonis M. Antihypertensive medications for risk reduction of first and recurrent ischemic stroke. Expert Rev Cardiovasc Ther. 2004; 2:867–876. [PubMed: 15500432]
62. Patnaik M, Pati P, Swain SN, Mohapatra MK, Dwibedi B, Kar SK, Ranjit M. Association of angiotensin-converting enzyme and angiotensin-converting enzyme-2 gene polymorphisms with essential hypertension in the population of Odisha, India. Ann Hum Biol. 2013 Epub ahead of print.
63. Pena Silva RA, Chu Y, Miller JD, Mitchell IJ, Penninger JM, Faraci FM, Heistad DD. Impact of ACE2 deficiency and oxidative stress on cerebrovascular function with aging. Stroke. 2012; 43:3358–3363. [PubMed: 23160880]
64. Pirkle JL, Freedman BI. Hypertension and chronic kidney disease: controversies in pathogenesis and treatment. Minerva urologica e nefrologica = The Italian journal of urology and nephrology. 2013; 65:37–50. [PubMed: 23538309]
65. Qin L, Crews FT. NADPH oxidase and reactive oxygen species contribute to alcohol-induced microglial activation and neurodegeneration. J Neuroinflammation. 2012; 9:5. [PubMed: 22240163]
66. Rashid P, Leonardi-Bee J, Bath P. Blood pressure reduction and secondary prevention of stroke and other vascular events - A systematic review. Stroke. 2003; 34:2741–2748. [PubMed: 14576382]

67. Regenhardt RW, Desland F, Mecca AP, Pioquinto DJ, Afzal A, Mocco J, Sumners C. Anti-inflammatory effects of angiotensin-(1-7) in ischemic stroke. Neuropharmacology. 2013; 71:154–163. [PubMed: 23583926]
68. Reinehr R, Gorg B, Becker S, Qvartskhava N, Bidmon HJ, Selbach O, Haas HL, Schliess F, Haussinger D. Hypoosmotic swelling and ammonia increase oxidative stress by NADPH oxidase in cultured astrocytes and vital brain slices. Glia. 2007; 55:758–771. [PubMed: 17352382]
69. Ren Z, Raucci FJ Jr, Browe DM, Baumgarten CM. Regulation of swelling-activated Cl(−) current by angiotensin II signalling and NADPH oxidase in rabbit ventricle. Cardiovasc Res. 2008; 77:73–80. [PubMed: 18006461]
70. Roks AJ, van Geel PP, Pinto YM, Buikema H, Henning RH, de Zeeuw D, van Gilst WH. Angiotensin-(1-7) is a modulator of the human renin-angiotensin system. Hypertension. 1999; 34:296–301. [PubMed: 10454457]
71. Santos RA, Simoes e Silva AC, Maric C, Silva DM, Machado RP, de Buhr I, Heringer-Walther S, Pinheiro SV, Lopes MT, Bader M, Mendes EP, Lemos VS, Campagnole-Santos MJ, Schultheiss HP, Speth R, Walther T. Angiotensin-(1-7) is an endogenous ligand for the G protein-coupled receptor Mas. Proceedings of the National Academy of Sciences of the United States of America. 2003; 100:8258–8263. [PubMed: 12829792]
72. Serrander L, Cartier L, Bedard K, Banfi B, Lardy B, Plastre O, Sienkiewicz A, Forro L, Schlegel W, Krause KH. NOX4 activity is determined by mRNA levels and reveals a unique pattern of ROS generation. Biochem J. 2007; 406:105–114. [PubMed: 17501721]
73. SHEP-Cooperative-Research-Group . Prevention of stroke by antihypertensive drug treatment in older persons with isolated systolic hypertension. Final results of the Systolic Hypertension in the Elderly Program (SHEP). JAMA : The Journal of the American Medical Association. 1991; 265:3255–3264. [PubMed: 2046107]
74. Sheth KN. Novel Approaches to the Primary Prevention of Edema After Ischemia. Stroke. 2013; 44:S136. [PubMed: 23709712]
75. Sica DA, Gehr TW. The pharmacokinetics and pharmacodynamics of angiotensin-receptor blockers in end-stage renal disease. J Renin Angiotensin Aldosterone Syst. 2002; 3:247–254. [PubMed: 12584668]
76. Stornetta RL, Hawelu-Johnson CL, Guyenet PG, Lynch KR. Astrocytes synthesize angiotensinogen in brain. Science. 1988; 242:1444–1446. [PubMed: 3201232]
77. Sukumaran V, Watanabe K, Veeraveedu PT, Gurusamy N, Ma M, Thandavarayan RA, Lakshmanan AP, Yamaguchi K, Suzuki K, Kodama M. Olmesartan, an AT1 antagonist, attenuates oxidative stress, endoplasmic reticulum stress and cardiac inflammatory mediators in rats with heart failure induced by experimental autoimmune myocarditis. Int J Biol Sci. 2011; 7:154–167. [PubMed: 21383952]
78. Tejada-Simon MV, Serrano F, Villasana LE, Kanterewicz BI, Wu GY, Quinn MT, Klann E. Synaptic localization of a functional NADPH oxidase in the mouse hippocampus. Mol Cell Neurosci. 2005; 29:97–106. [PubMed: 15866050]
79. Tucker B, Olson JE. Glutamate receptor-mediated taurine release from the hippocampus during oxidative stress. J Biomed Sci. 2010; 17(Suppl 1):S10. [PubMed: 20804584]
80. Turner DA, Aitken PG, Somjen GG. Optical mapping of translucence changes in rat hippocampal slices during hypoxia. Neurosci Lett. 1995; 195:209–213. [PubMed: 8584212]
81. Vallet P, Charnay Y, Steger K, Ogier-Denis E, Kovari E, Herrmann F, Michel JP, Szanto I. Neuronal expression of the NADPH oxidase NOX4, and its regulation in mouse experimental brain ischemia. Neuroscience. 2005; 132:233–238. [PubMed: 15802177]
82. von Bohlen und Halbach O. The renin-angiotensin system in the mammalian central nervous system. Curr Protein Pept Sci. 2005; 6:355–371. [PubMed: 16101434]
83. von Sarnowski B, Putaala J, Grittner U, Gaertner B, Schminke U, Curtze S, Huber R, Tanislav C, Lichy C, Demarin V, Basic-Kes V, Ringelstein EB, Neumann-Haefelin T, Enzinger C, Fazekas F, Rothwell PM, Dichgans M, Jungehulsing GJ, Heuschmann PU, Kaps M, Norrving B, Rolfs A, Kessler C, Tatlisumak T. Lifestyle risk factors for ischemic stroke and transient ischemic attack in young adults in the Stroke in Young Fabry Patients study. Stroke. 2013; 44:119–125. [PubMed: 23150649]

84. Walder CE, Green SP, Darbonne WC, Mathias J, Rae J, Dinauer MC, Curnutte JT, Thomas GR. Ischemic stroke injury is reduced in mice lacking a functional NADPH oxidase. Stroke. 1997; 28:2252–2258. [PubMed: 9368573]
85. Wang G, Coleman CG, Chan J, Faraco G, Marques-Lopes J, Milner TA, Guruju MR, Anrather J, Davisson RL, Iadecola C, Pickel VM. Angiotensin II slow-pressor hypertension enhances NMDA currents and NOX2-dependent superoxide production in hypothalamic paraventricular neurons. American Journal of Physiology - Regulatory, Integrative and Comparative Physiology. 2013; 304:R1096–R1106.
86. Wardman P. Fluorescent and luminescent probes for measurement of oxidative and nitrosative species in cells and tissues: progress, pitfalls, and prospects. Free Radic Biol Med. 2007; 43:995–1022. [PubMed: 17761297]
87. Wright JW, Kramar EA, Meighan SE, Harding JW. Extracellular matrix molecules, long-term potentiation, memory consolidation and the brain angiotensin system. Peptides. 2002; 23:221–246. [PubMed: 11814638]
88. Xia H, Feng Y, Obr TD, Hickman PJ, Lazartigues E. Angiotensin II type 1 receptor-mediated reduction of angiotensin-converting enzyme 2 activity in the brain impairs baroreflex function in hypertensive mice. Hypertension. 2009; 53:210–216. [PubMed: 19124678]
89. Xia H, Suda S, Bindom S, Feng Y, Gurley SB, Seth D, Navar LG, Lazartigues E. ACE2-mediated reduction of oxidative stress in the central nervous system is associated with improvement of autonomic function. PLoS One. 2011; 6:e22682. [PubMed: 21818366]
90. Xu P, Sriramula S, Lazartigues E. ACE2/ANG-(1-7)/Mas pathway in the brain: the axis of good. Am J Physiol Regul Integr Comp Physiol. 2011; 300:R804–817. [PubMed: 21178125]
91. Yang G, Gray TS, Sigmund CD, Cassell MD. The angiotensinogen gene is expressed in both astrocytes and neurons in murine central nervous system. Brain research. 1999; 817:123–131. [PubMed: 9889347]
92. Yang L, Wang H, Shah K, Karamyan VT, Abbruscato TJ. Opioid receptor agonists reduce brain edema in stroke. Brain research. 2011; 1383:307–316. [PubMed: 21281614]
93. Zawada WM, Banninger GP, Thornton J, Marriott B, Cantu D, Rachubinski AL, Das M, Griffin WS, Jones SM. Generation of reactive oxygen species in 1-methyl-4-phenylpyridinium (MPP+) treated dopaminergic neurons occurs as an NADPH oxidase-dependent two-wave cascade. J Neuroinflammation. 2011; 8:129. [PubMed: 21975039]
94. Zhang H, Schmeisser A, Garlichs CD, Plotze K, Damme U, Mugge A, Daniel WG. Angiotensin II-induced superoxide anion generation in human vascular endothelial cells: role of membrane-bound NADH-/NADPH-oxidases. Cardiovasc Res. 1999; 44:215–222. [PubMed: 10615405]
95. Zimmerman MC, Lazartigues E, Lang JA, Sinnayah P, Ahmad IM, Spitz DR, Davisson RL. Superoxide mediates the actions of angiotensin II in the central nervous system. Circ Res. 2002; 91:1038–1045. [PubMed: 12456490]
96. Zimmerman MC, Lazartigues E, Sharma RV, Davisson RL. Hypertension caused by angiotensin II infusion involves increased superoxide production in the central nervous system. Circ Res. 2004; 95:210–216. [PubMed: 15192025]

Bullet Highlights

We used brain slices from transgenic mice with features of human essential hypertension

Brain slices were exposed to oxygen-glucose deprivation (OGD) to model ischemic stroke

Overexpression of ACE2 in neurons reduces NADPH oxidase expression, ROS production, and brain cell damage following OGD

ACE2 protects brain by activating the ACE2/Ang-(1-7)/Mas signaling axis which opposes actions of the ACE/Ang II/AT1R axis

Mas receptor activation can be neuroprotective for stroke in hypertensive patients

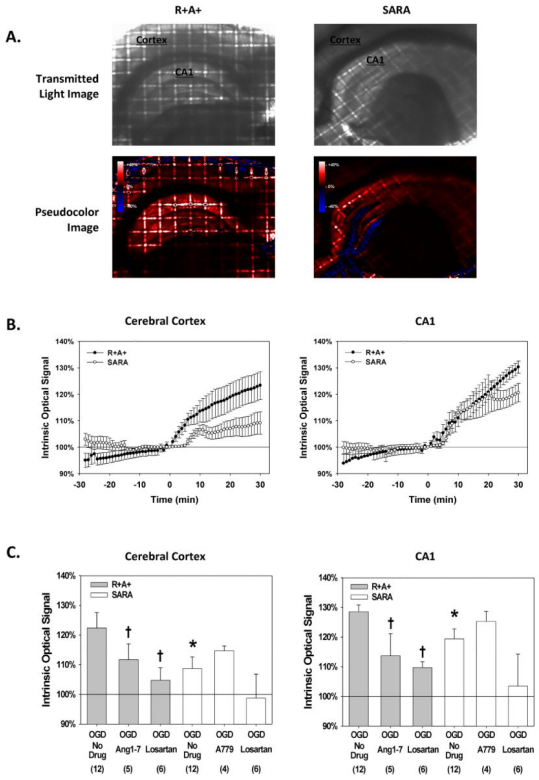

Figure 1.

Tissue swelling during oxygen and glucose deprivation (OGD) exposure. Brain slices were perfused with control aCSF until OGD exposure was initiated at time t=0 min. **A.** Representative images of brain slices from R+A+ and SARA animals. For each pair of images the top panel is the transmitted light image prior to OGD exposure. The hippocampal CA1 region and cerebral cortex are labeled for anatomical reference. The lower panel is a pseudocolor image of the same slice showing percent changes in light transmission after 30 min of OGD calculated on a pixel-by-pixel basis. A color calibration scale for the magnitude of the change in light transmission is shown in the figure insets. **B.** Mean IOS values from R+A+ and SARA animals before and during OGD exposure measured from regions of interest in cerebral cortex and hippocampal CA1 region. IOS is defined as the intensity of transmitted light during OGD treatment expressed as a percent of the value measured prior to the start of OGD. Values are the mean ± SEM for slices from 12 animals **C.** IOS values measured in cerebral cortex and the hippocampal CA1 region after 30 min of IOS exposure for brain slices from R+A+ and SARA animals with and without various drug treatments. The mean IOS from regions of interest in the cerebral cortex and hippocampal CA1 region for the final 5 images during OGD exposure was calculated for each slice and these results averaged to give the mean ± SEM values shown. The number of animals for each group is in the parentheses. Log-transformed data were analyzed by ANOVA with *post hoc* Dunnett's test. For slices from SARA animals given no drug treatment, * indicates values that were significantly different from that measured in slices from R+A+ animals with no drug treatment. † indicates values significantly different from those measured in slices from animals of the same genotype with no drug treatment.

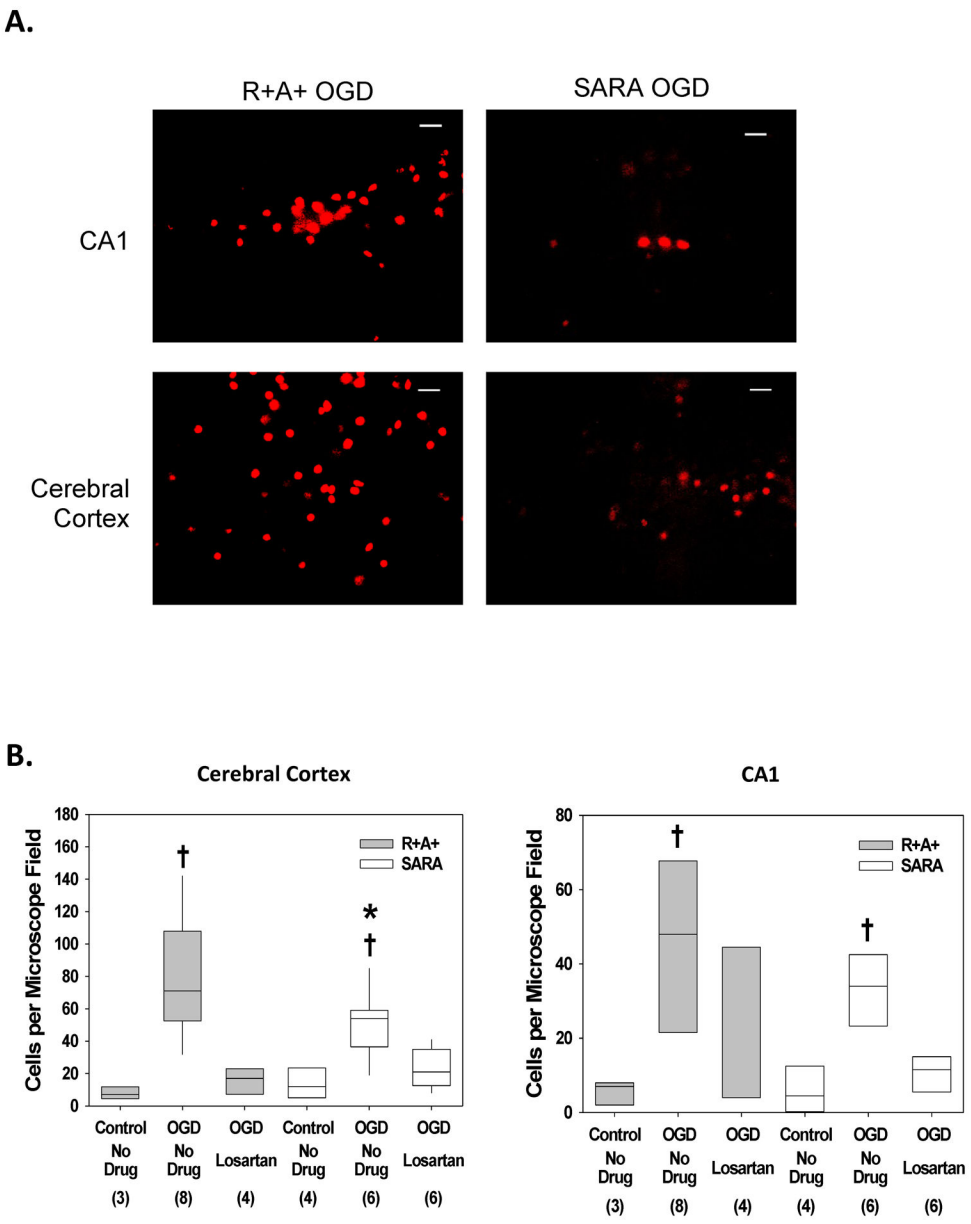

Figure 2.

ROS production during oxygen and glucose deprivation (OGD) exposure. Slices were exposed to DHE for 30 min during control or OGD conditions. Some slices also were treated with losartan during OGD exposure. **A.** Epifluorescence images of cerebral cortex and the hippocampal CA1 region of slices from R+A+ and SARA animals showing DHE-positive cells following OGD exposure. The entire microscope field is shown in these images with the scale bar indicating 25 μm. **B.** Cell counts of DHE-positive cells in cerebral cortex and hippocampal CA1 region. Boxes designate the interquartile range with the horizontal line indicating the median cell counts for the number of animals shown in parentheses. 95th and 5th percentiles are indicated with vertical lines where possible. Data were analyzed by Kruskal-Wallis One-Way ANOVA and Newman-Keuls test for multiple

comparisons. For slices from SARA animals, * indicates values significantly different from those measured in slices from R+A+ animals exposed to the same perfusion conditions. † indicates values significantly different from those measured in slices from animals of the same genotype under control conditions.

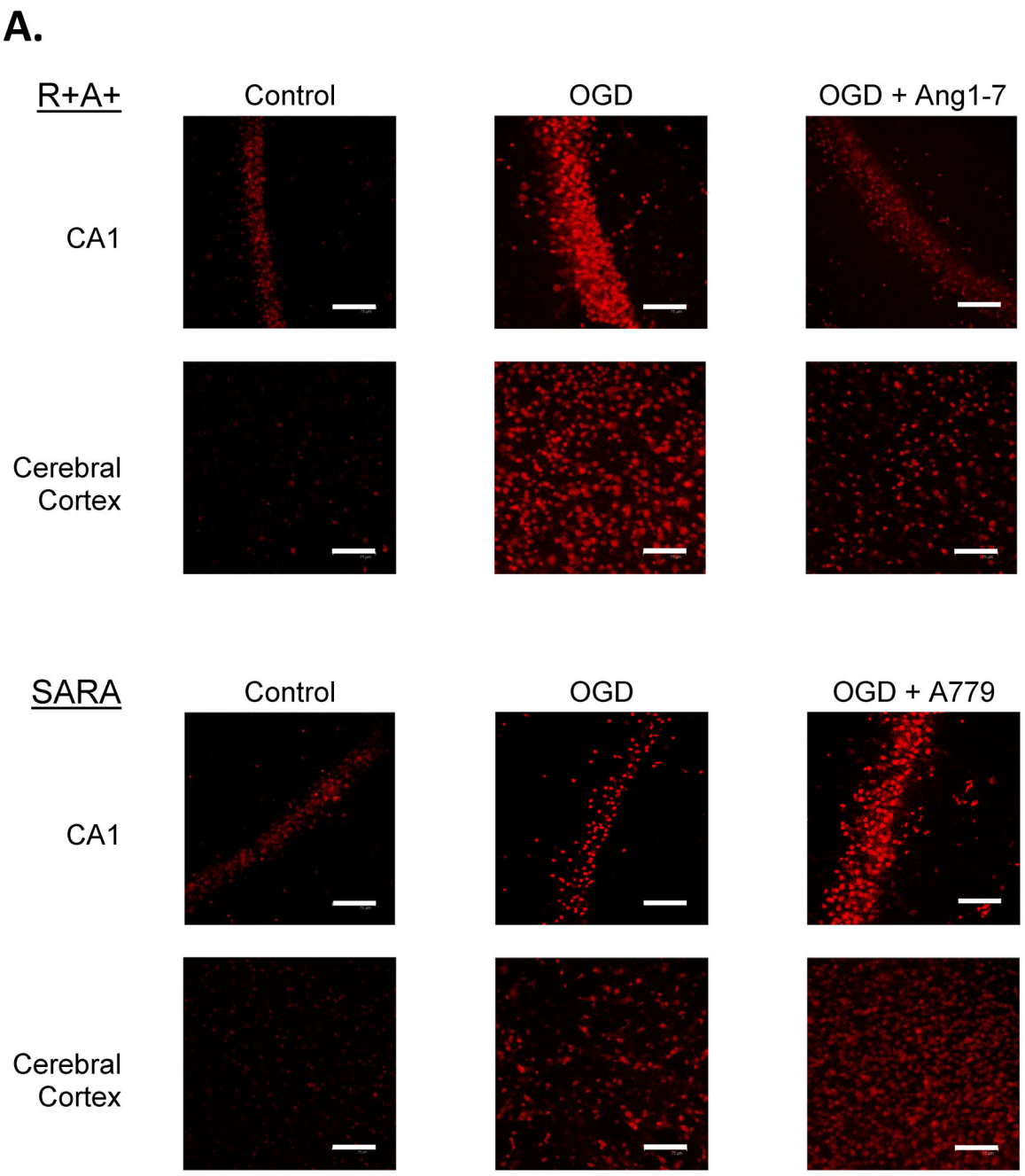

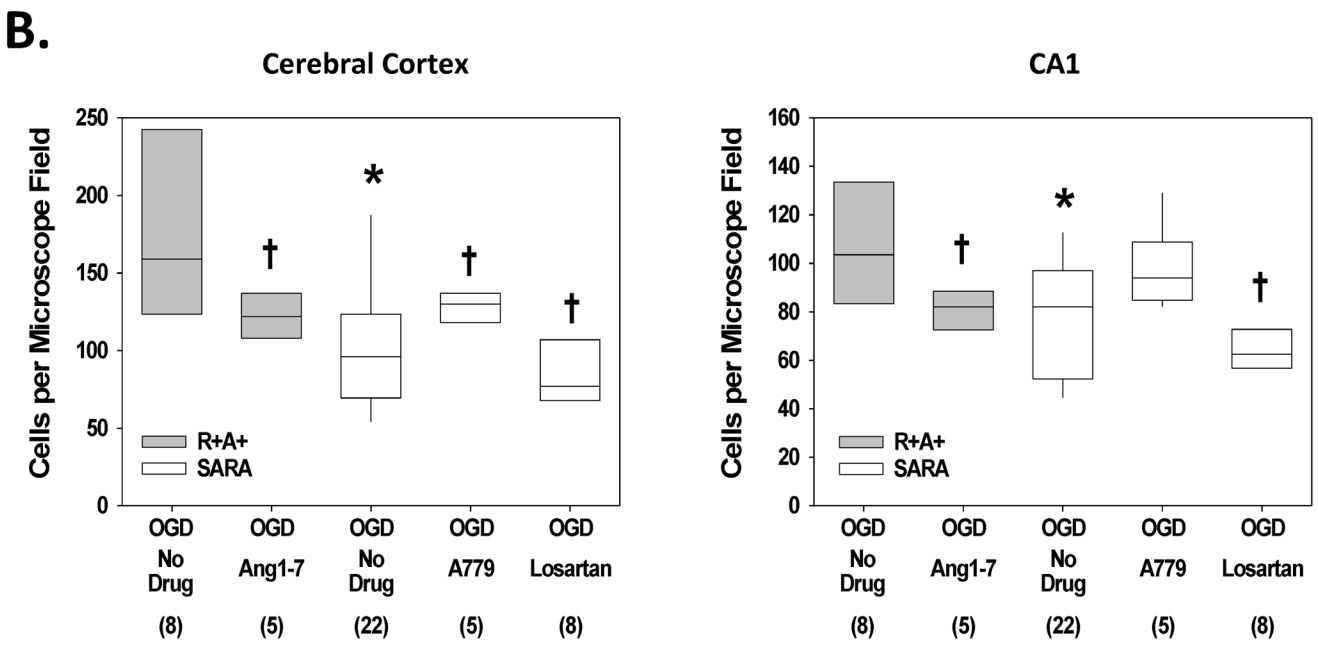

Figure 3.

Cell death following oxygen and glucose deprivation (OGD) exposure. Slices were exposed to control aCSF or OGD for 30 min and then stained with PI for 15 min. Some slices had drug treatments during OGD as indicated. **A.** Confocal images of cerebral cortex and hippocampal CA1 region of slices from R+A+ and SARA animals following 30 min perfusion with control or OGD conditions. The entire microscope field is shown in these images with scale bar indicating 75 μm. **B.** Cell counts of PI-positive cells in cerebral cortex and hippocampal CA1 region. Boxes designate the interquartile range with the horizontal line indicating the median of cell counts for the number of animals shown in parentheses. 95^{th} and 5^{th} percentiles are indicated with vertical lines where possible. Data were analyzed by Kruskal-Wallis One-Way ANOVA and Newman-Keuls test for multiple comparisons. For slices given no drug treatment, * indicates values significantly different from those measured in slices from R+A+ animals. † indicates values significantly different from those measured in slices from animals of the same genotype with no drug treatment.

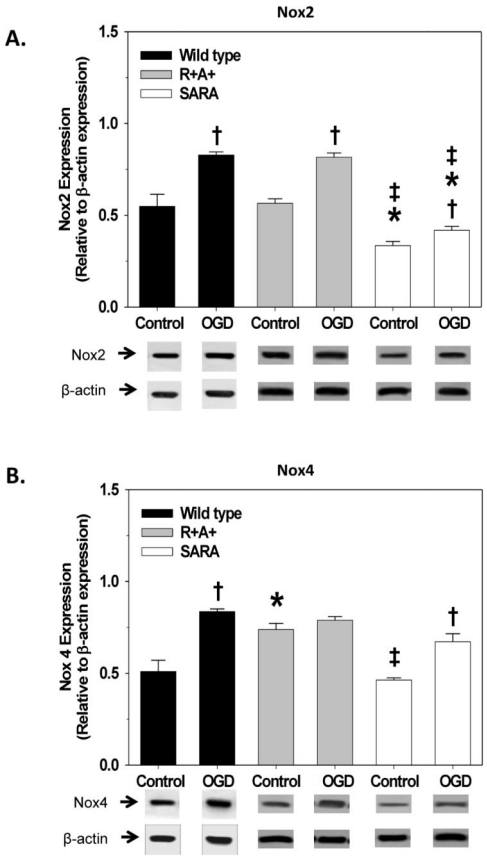

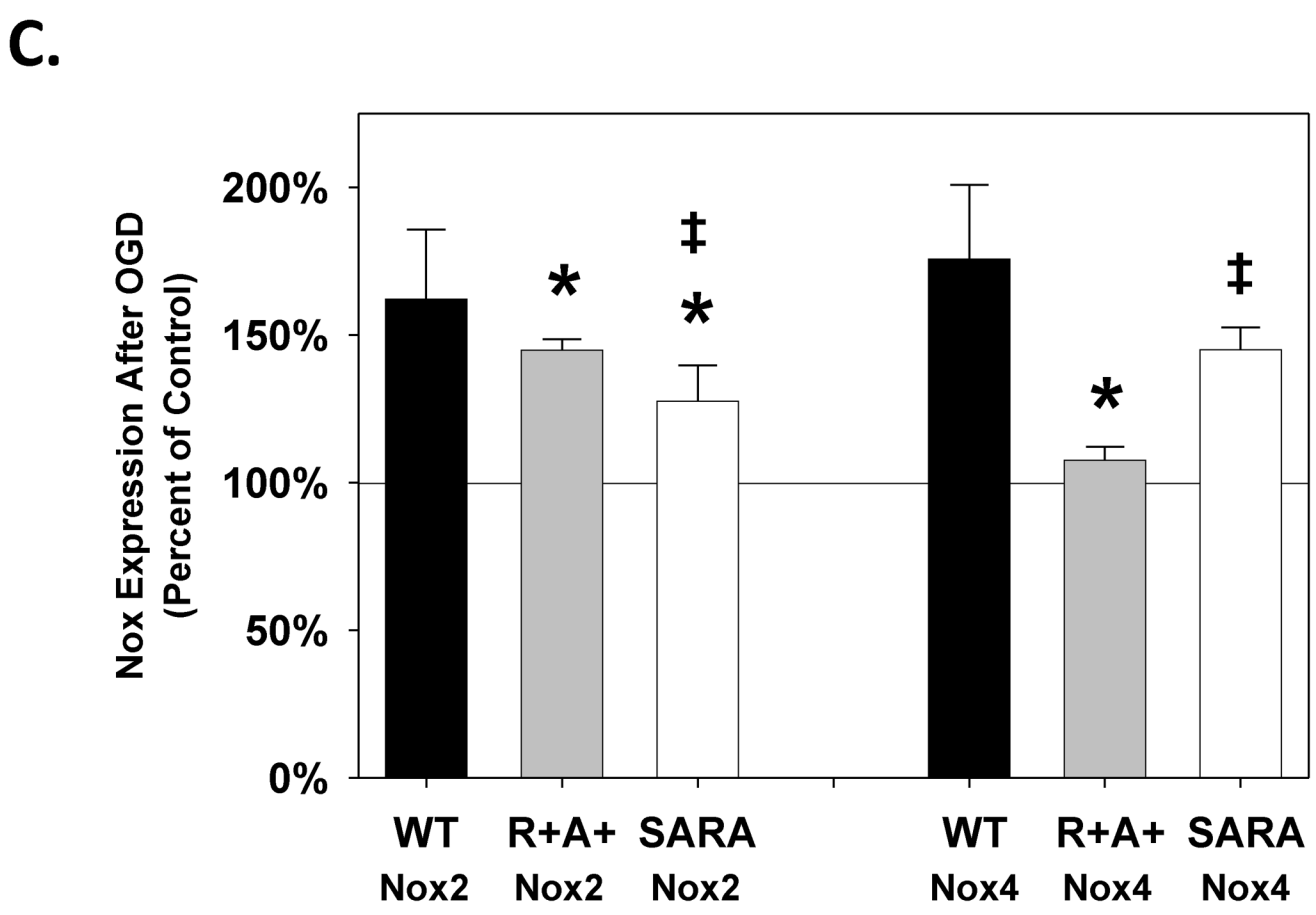

Figure 4.

Nox2 and Nox4 expression following oxygen and glucose deprivation (OGD) exposure. Slices were perfused with control aCSF or OGD conditions for 30 min and then prepared for western blot analysis. Expression levels of Nox2 (**A**) and Nox4 (**B**) in brain slices from wild type (WT), R+A+, and SARA animals following control or OGD exposure are shown relative to expression levels of β-actin. **C** shows Nox expression in brain slices following OGD as a percent of the expression measured contemporaneously in brain slices from the same animal exposed to control conditions. Values are the mean ± SEM of data from 5 R+A + animals, 5 wild type animals, and 4 SARA animals. Representative bands from western blots for Nox2, Nox4, and β-actin are shown under each bar in **A** and **B**. Data were analyzed by ANOVA with *post hoc* Neuman-Keuls test for multiple comparisons. * indicates values which are significantly different from those measured slices from wild type animals given the same perfusion treatment. † indicates values which are significantly different from those measured in slices from animals of the same genotype exposed to control conditions. For slices from SARA animals, ‡ indicates values which are significantly different from those measured in slices from R+A+ animals exposed to the same perfusion treatment.